# Micromechanics Based Composite Material Model for Impact and Crashworthiness Explicit Finite Element Simulation

Ala Tabiei♦ and Quing Chen[1]
CENTER OF EXCELLENCE IN DYNA3D ANALYSIS[2]
Department of Aerospace Eng. & Eng. Mechanics
University of Cincinnati, Cincinnati, OH 45221-0070

**Abstract**
A micro-mechanical model is developed for laminated composite materials and implemented in the explicit finite element method. The objective of this study is to get an accurate and simple micro-model, which can be used in the displacement-based nonlinear explicit finite element code DYNA3D. The micro-mechanical model implemented in the explicit finite element code can be used for simulating the behavior of composite structures under various loads such as impact and crash. The stress-strain relation for the micro-model is derived for shell element. Micro Failure Criterion (MFC) is presented for each material constituent and failure mode. The implemented model is validated through several test examples. As a demonstration case of the stability of the developed micro-model a finite element model of Graphite/Epoxy tube structure is developed and simulated under axial crash.

**Nomenclature**

| | |
|---|---|
| [S] | Compliance matrix |
| [Q] | Reduced stiffness matrix |
| [C] | Stiffness Matrix |
| $\sigma_{ij}$ | Stress tensor |
| $\varepsilon_{ij}$ | Strain tensor |
| $D_i$ | Stiffness reduction factor |
| $G_m$ | In-plane shear modulus for matrix |
| $G_{12f}$ | In-plane shear modulus for fiber |
| $E_1$ | Tensile modulus for fiber (along fiber direction) |
| $E_2$ | Tensile modulus for fiber (normal to fiber direction) |
| $E_m$ | Tensile modulus for matrix |
| $\nu$ | Poisson Ratio |
| $E_x$ | Tensile modulus for unit cell (along fiber direction) |
| $E_y$ | Tensile modulus for unit cell (normal to fiber direction) |
| $X_t$ | Tensile strength for unit cell (along fiber direction ) |
| $X_c$ | Compression strength for unit cell (along fiber direction) |
| $Y_t$ | Tensile strength for unit cell (normal to fiber direction) |
| $Y_c$ | Compression strength for unit cell (normal to fiber direction) |
| S | In-plane shear strength for unit cell |
| $X_t^{(f)}$ | Tensile strength for fiber |
| $Y_t^{(m)}$ | Tensile strength for matrix |
| $Y_c^{(m)}$ | Compression strength for matrix |
| $S^{(m)}$ | In-plane shear strength for matrix |

♦ Director.
[1] Graduate Research Assistant
[2] www.ase.uc.edu/~atabiei

## Introduction

A composite material is one composed of two or more distinct material constituents, that are mechanically combined in a way to produce a material with properties not achievable by any of the elemental constituents acting alone. Composite materials are ideally suited for products and applications where high stiffness-to-weight and strength-to weight ratios are desirable, such as in automotive, aircraft, and spacecraft structures. Composites are resistant to corrosion and fatigue, and typically have good impact tolerance. All these attributes make the use of composites an attractive option for a wide range of applications, and consequently there has been a steady rise in the use of composites in the aerospace industry, automobile industry, and sporting goods industry.

Recently, computational micro-mechanical studies have become increasingly valuable as the awareness and requirement for more efficient design increases. The substantial time and cost for performance of full-scale tests makes it attractive to perform as much of the micro-mechanical evaluation as possible using numerical simulation. These simulations, coupled with a limited number of well-planned sub-scale and full-scale tests, offer tremendous savings of time and money. The rapid growth in computational speed has made complex simulations feasible. This is particularly true, where explicit integration finite element codes are utilized. Explicit integration of the material point allows the equations of motion to be decoupled, though requires very small time steps to maintain numerical stability. And even with very large models the computer memory demands are small since no global stiffness matrix is inverted.

The earliest study of micro-mechanics for general structural analysis of composites is by Bahei-El-Din et al. [1]. The Vanishing Fiber Diameter (VFD) model was employed in a three-dimensional finite element analysis program to model the response of laminate plates. The matrix material was described by the von Mises yield criterion with the Prager-Ziegler kinematics-hardening rule. The result showed fair agreement with experiments and with detailed finite element solutions. The strains in the fiber direction were well predicted; But the strain in the transverse direction were over-predicted, which is a characteristic of the VFD micro-model.

Adams and Crane [2] used the finite element method to study the response of a representative volume element of a composite lamina. Nonlinear behavior of the matrix was taken into account. This micro-mechanical model was in conjunction with Classical Laminate Plate Theory to determine the nonlinear response of simple laminates. It's one of the first attempts at incorporating micro-mechanics into structural analysis for composites. But it requires extensive computational resources and is expensive.

In the above works, too much computational work is involved, makes the approach too expensive. So in this study, a simpler micro-model proposed by Pecknold et al. [3] is investigated.

Composites can be viewed and analyzed at different levels and on different scales, depending on the particular characteristics and behavior under consideration.

At the constituent level, micro-mechanics is the study of the interaction of the constituents. It deals with the state of deformation and stress in the constituents and local failures, such as matrix failure (tensile, compressive, shear), fiber failure (tensile, buckling, splitting), and interface failure (debonding). Micro-mechanics is particularly important in the study of properties such as strength, fracture toughness, and fatigue life, which are strongly influenced by local characteristics that cannot be integrated or averaged. Micro-mechanics also allows the prediction of average behavior at the lamia level as a function of constituent properties and local conditions.

One advantage of using a micro-mechanical theory is that no appropriate knowledge of the lamina response is needed, since this response is predicted from the properties of the

constituent fiber and matrix phase. The constituents themselves are homogeneous, and the vast amount of knowledge accumulated regarding the behavior of homogeneous materials can be directly employed to construct the effective response of a composite lamina. A second advantage is that since only the properties of the constituents are required, the effect of using different fiber matrix combinations and different fiber volume fractions can be easily studied. Also, the interaction of the fiber and the matrix material can be accurately modeled.

**Constitutive Equations for Composite Materials**

The constitutive equations used to model the behavior of composite materials may be classified as Micro-mechanical or Macro-mechanical in nature. The primary advantage of macro-mechanical equations is that they require less computational work. These equations are adequate to describe response due to mechanical loading. But, it still needs to be developed more for complex load histories, strain rate sensitivity and creep etc. Micro-mechanical constitutive equations require more computational work, and each constituent property has to be determined by experimental tests. However, the advantage is in these cases, like complex load history, strain rate sensitivity and creep, can be studied with less difficulty. In macro-mechanical analyses of laminate, a lamina is modeled as an anisotropic homogeneous material and therefore it can not give information about the state of stress and strain in the constituent. In the following section, the micro-model is presented in more details.
In application of finite element method for analysis of the global behavior of thin-walled structures made of laminated composites, shell elements are usually employed. The required constitutive laws are generally written as follows:

$$\begin{Bmatrix} \varepsilon_{11} \\ \varepsilon_{22} \\ \gamma_{12} \end{Bmatrix} = \begin{bmatrix} S_{11} & S_{12} & 0 \\ S_{12} & S_{22} & 0 \\ 0 & 0 & S_{66} \end{bmatrix} \begin{Bmatrix} \sigma_{11} \\ \sigma_{22} \\ \sigma_{12} \end{Bmatrix} \tag{1}$$

and

$$\begin{Bmatrix} \gamma_{23} \\ \gamma_{13} \end{Bmatrix} = \begin{bmatrix} S_{44} & 0 \\ 0 & S_{55} \end{bmatrix} \begin{Bmatrix} \sigma_{23} \\ \sigma_{13} \end{Bmatrix} \tag{2}$$

In these equations the global normal stress in thickness direction is ignored. During the incremental-iterative solution scheme, as used in finite element analysis of nonlinear problems, a change of the nodal displacements takes place. The displacement increment causes an increment of strain $\Delta\{\bar{\varepsilon}_i\}$ at a material point. The material model is required to calculate the incremental stress $\Delta\{\bar{\sigma}_i\}$. Stiffnesses, strains and stresses are tracked at the material points within each element. This information is provided by the micro-mechanics composite material model, which interfaces with the nonlinear explicit finite element code. The heterogeneous nature of the composite material is hidden from the main analysis code. Figure (1) shows a schematic of the micro-mechanical model and the interface with the finite element code. The actual laminated composite is replaced by an equivalent homogenous material whose properties are determined by requiring that the actual material and the equivalent material behave in the same way when subjected to certain stresses or strains. The interface consists of stresses and strains transfer between the material model and the analysis code. The main analysis code only sees this equivalent homogenous anisotropic material.

**Micro-Mechanics Constitutive Model**

In this study the model proposed by Pecknold et al. [3] is employed. The micro-model considers the response of a unidirectional lamina, starting from the fiber and matrix constitutive descriptions. We can consider a lamina transversely isotropic with the 2-3 plane (normal to the fibers) as the plane of isotropy. In the present study the following assumptions are considered as below:

i) The fiber material is homogeneous and linearly elastic;
ii) The matrix material is homogeneous and linearly elastic;
iii) The fiber positioning in the matrix material is such that the resulting lamina material is macro-mechanically-homogeneous material with linearly elastic behavior.
iv) There is a complete and strong bond at the interface of the constituent materials.

The proposed micro-model is based on the assumption that the internal microstructure of the lamina consists of square fibers. Shown in the lower portion of figure (1) is the representative unit cell, which is an assumed geometry of the idealized composite. The unit cell is divided into three sub-cells; one sub-cell is fiber, denoted as **f**, and two matrix sub-cells, denoted as $\mathbf{M_A}$ and $\mathbf{M_B}$ respectively. The three sub-cells are grouped into two parts: Material Part **A**, consists of the fiber sub-cell **f** and the series-or-parallel connected matrix sub-cell $\mathbf{M_A}$. Material Part **B** consists of the remaining matrix $\mathbf{M_B}$. The dimensions of the unit cell are 1x1 unit square. The dimensions of fiber and matrix sub-cells are denoted by $W_f$ and $W_m$ respectively as shown in figure (1) and defined as below.

$$\begin{aligned} W_f &= \sqrt{V_f} \\ W_m &= 1 - W_f \end{aligned} \tag{3}$$

Where $V_f$ is the Fiber Volume Fraction. The effective stresses and strains in the lamina are determined from the sub-cell values in two phases: first, fiber **f** and matrix $\mathbf{M_A}$ construct Part A; then Part A and Part B construct the unidirectional lamina. The homogenized stresses and strains in Part A is given by the following equation:

$$\begin{aligned} &\begin{Bmatrix} \varepsilon_{11} \\ \sigma_{22} \\ \sigma_{12} \end{Bmatrix}_A = \begin{Bmatrix} \varepsilon_{11} \\ \sigma_{22} \\ \sigma_{12} \end{Bmatrix}_f = \begin{Bmatrix} \varepsilon_{11} \\ \sigma_{22} \\ \sigma_{12} \end{Bmatrix}_{M_A} \\ &\begin{Bmatrix} \sigma_{11} \\ \varepsilon_{22} \\ \varepsilon_{12} \end{Bmatrix}_A = W_f \begin{Bmatrix} \sigma_{11} \\ \varepsilon_{22} \\ \varepsilon_{12} \end{Bmatrix}_f + W_m \begin{Bmatrix} \sigma_{11} \\ \varepsilon_{22} \\ \varepsilon_{12} \end{Bmatrix}_{M_A} \end{aligned} \tag{4}$$

In the above the analogy shown in figure (2) is used for the various components. Therefore the homogenized stresses and strains in the Unit Cell is given by the following:

$$\begin{aligned} &\begin{Bmatrix} \varepsilon_{11} \\ \varepsilon_{22} \\ \varepsilon_{12} \end{Bmatrix}_C = \begin{Bmatrix} \varepsilon_{11} \\ \varepsilon_{22} \\ \varepsilon_{12} \end{Bmatrix}_B = \begin{Bmatrix} \varepsilon_{11} \\ \varepsilon_{22} \\ \varepsilon_{12} \end{Bmatrix}_A \\ &\begin{Bmatrix} \sigma_{11} \\ \sigma_{22} \\ \sigma_{12} \end{Bmatrix}_C = W_f \begin{Bmatrix} \sigma_{11} \\ \sigma_{22} \\ \sigma_{12} \end{Bmatrix}_A + W_m \begin{Bmatrix} \sigma_{11} \\ \sigma_{22} \\ \sigma_{12} \end{Bmatrix}_B \end{aligned} \tag{5}$$

**Constitutive Matrices and Stress Update for the Micro-Model**

Part B is a homogeneous isotropic matrix (resin) material. The compliance matrix is given by the following:

$$[S]_B = \begin{Bmatrix} \frac{1}{E_m} & \frac{-\upsilon_m}{E_m} & 0 \\ \frac{-\upsilon_m}{E_m} & \frac{1}{E_m} & 0 \\ 0 & 0 & \frac{1}{G_m} \end{Bmatrix} \tag{6}$$

and therefore the stiffness matrix is

$$[Q]_B = [S]_B^{-1} = \begin{Bmatrix} \frac{E_m}{1-\upsilon_m^2} & \frac{\upsilon_m E_m}{1-\upsilon_m^2} & 0 \\ \frac{\upsilon_m E_m}{1-\upsilon_m^2} & \frac{E_m}{1-\upsilon_m^2} & 0 \\ 0 & 0 & G_m \end{Bmatrix} \tag{7}$$

The stress increment is related to the strain increment and the total stress is obtained from the following:

$$\begin{aligned} \{\Delta\sigma\}_B &= [Q]_B \cdot \{\Delta\varepsilon\}_B \\ \{\sigma\}_B^{new} &= \{\sigma\}_B^{old} + \{\Delta\sigma\}_B \end{aligned} \tag{8}$$

Part A consists of an isotropic matrix sub-cell $\mathbf{M_A}$ and an orthotropic fiber sub-cell **f**. The compliance matrix for $\mathbf{M_A}$ is given by the following equation:

$$[S]_{M_A} = \begin{Bmatrix} \frac{1}{E_m} & \frac{-\upsilon_m}{E_m} & 0 \\ \frac{-\upsilon_m}{E_m} & \frac{1}{E_m} & 0 \\ 0 & 0 & \frac{1}{G_m} \end{Bmatrix} \tag{9}$$

$$[Q]_{M_A} = [S]_{M_A}^{-1} = \begin{Bmatrix} \frac{E_m}{1-\upsilon_m^2} & \frac{\upsilon_m E_m}{1-\upsilon_m^2} & 0 \\ \frac{\upsilon_m E_m}{1-\upsilon_m^2} & \frac{E_m}{1-\upsilon_m^2} & 0 \\ 0 & 0 & G_m \end{Bmatrix} \tag{10}$$

The stress increment is related to the strain increment and the total stress is obtained from the following:

$$\{\Delta\sigma\}_{M_A} = [Q]_{M_A} \cdot \{\Delta\varepsilon\}_{M_A}$$
$$\{\sigma\}^{new}_{M_A} = \{\sigma\}^{old}_{M_A} + \{\Delta\sigma\}_{M_A} \tag{11}$$

Sub-cell **f** is the fiber portion of the unit cell and the compliance matrix is given by the following equation:

$$[S]_f = \begin{Bmatrix} \frac{1}{E_1} & \frac{-\upsilon_f}{E_1} & 0 \\ \frac{-\upsilon_f}{E_1} & \frac{1}{E_2} & 0 \\ 0 & 0 & \frac{1}{G_f} \end{Bmatrix} \tag{12}$$

$$[Q]_f = [S]_f^{-1} = \begin{Bmatrix} \frac{1}{E_2 F_f} & \frac{\upsilon_f}{E_1 F_f} & 0 \\ \frac{\upsilon_f}{E_1 F_f} & \frac{\upsilon_f}{E_1 F_f} & 0 \\ 0 & 0 & G_f \end{Bmatrix} \tag{13}$$

where

$$F_f = \frac{1}{E_1 E_2} - \frac{\upsilon_f^{\,2}}{E_1^{\,2}}$$

The stress increment is related to the strain increment and the total stress is obtained from the following:

$$\{\Delta\sigma\}_f = [Q]_f \cdot \{\Delta\varepsilon\}_f$$
$$\{\sigma\}^{new}_f = \{\sigma\}^{old}_f + \{\Delta\sigma\}_f \tag{14}$$

So, finally for Part A, we have the following:

$$\begin{Bmatrix} \sigma_{22} \\ \sigma_{12} \end{Bmatrix}_A = \begin{Bmatrix} \sigma_{22} \\ \sigma_{12} \end{Bmatrix}_f$$
$$\{\sigma_{11}\}_A = W_f \{\sigma_{11}\}_f + W_m \{\sigma_{11}\}_{M_A} \tag{15}$$

The incremental and total stresses for UNIT CELL are finally obtained from the following:

$$\begin{Bmatrix}\Delta\sigma_{11}\\ \Delta\sigma_{22}\\ \Delta\sigma_{12}\end{Bmatrix}_C = W_f\begin{Bmatrix}\Delta\sigma_{11}\\ \Delta\sigma_{22}\\ \Delta\sigma_{12}\end{Bmatrix}_A + W_m\begin{Bmatrix}\Delta\sigma_{11}\\ \Delta\sigma_{22}\\ \Delta\sigma_{12}\end{Bmatrix}_B$$

$$\begin{Bmatrix}\sigma_{11}\\ \sigma_{22}\\ \sigma_{12}\end{Bmatrix}_{new} = \begin{Bmatrix}\sigma_{11}\\ \sigma_{22}\\ \sigma_{12}\end{Bmatrix}_{old} + \begin{Bmatrix}\Delta\sigma_{11}\\ \Delta\sigma_{22}\\ \Delta\sigma_{12}\end{Bmatrix}$$

(16)

The transverse shear stresses are given by the following equations:

$$\begin{Bmatrix}\Delta\sigma_{13}\\ \Delta\sigma_{23}\end{Bmatrix}_B = \begin{bmatrix}G_m & 0\\ 0 & G_m\end{bmatrix}\begin{Bmatrix}\Delta\varepsilon_{13}\\ \Delta\varepsilon_{23}\end{Bmatrix}_B \tag{17}$$

$$\begin{Bmatrix}\Delta\sigma_{13}\\ \Delta\sigma_{23}\end{Bmatrix}_A = \begin{bmatrix}\dfrac{1}{\dfrac{W_f}{G_{12}^f}+\dfrac{W_m}{G_m}} & 0\\ 0 & \dfrac{1}{\dfrac{W_f}{G_{12}^f}+\dfrac{W_m}{G_m}}\end{bmatrix}\begin{Bmatrix}\Delta\varepsilon_{13}\\ \Delta\varepsilon_{23}\end{Bmatrix}_A \tag{18}$$

and

$$\begin{Bmatrix}\Delta\sigma_{13}\\ \Delta\sigma_{23}\end{Bmatrix}_c = W_f\begin{Bmatrix}\Delta\sigma_{13}\\ \Delta\sigma_{23}\end{Bmatrix}_A + W_m\begin{Bmatrix}\Delta\sigma_{13}\\ \Delta\sigma_{23}\end{Bmatrix}$$

$$\begin{Bmatrix}\sigma_{13}\\ \sigma_{23}\end{Bmatrix}_{new} = \begin{Bmatrix}\sigma_{13}\\ \sigma_{23}\end{Bmatrix}_{old} + \begin{Bmatrix}\Delta\sigma_{13}\\ \Delta\sigma_{23}\end{Bmatrix} \tag{19}$$

**Failure Criteria**

Simple failure models for composite materials can be used to reliably predict the onset of failure, but not to predict the post-failure deformation, which are important in the impact analysis [4]. Complex composite damage models must be developed which account for a combination of several typical failure mechanisms: transverse matrix cracking, transverse matrix crashing, fiber breakage, fiber buckling, and matrix crashing in the fiber direction. These failure modes can be accounted for by employing micro-mechanical failure criteria (MFC) to model the progressive damage in the laminae.

The advantage of micromechanical model over a macromechanical model is that the stresses can be associated and related to each constituent (fiber and matrix). Therefore, failure can be identified in each of these constituents and the proper degradation in strength can be modeled. In this investigation the failure issue is addressed using criterion for each failure mode so that the basic important phenomenon can be captured and correlated with test observations.

When failure occurs, material will lose their load carrying capability in certain modes of deformation. To adequately model this behavior, the compliance matrix and stresses are modified according to the failure modes (see Tabiei et al [5] for details). To simulate failure in explicit finite element method, failure must be modeled by a gradual loss of stiffness in order to provide a stable solution instead of an instantaneous loss. A transition to the failed

condition is assumed to occur during a finite time. The failure criteria used in the model are as follows:

- Fiber fracture in tension occurs when the axial stress in fiber $\sigma_{11}^{f}$ is $\geq$ than the fiber tensile strength.
- Matrix shearing occurs when the max of ($\left|\tau_{12}^{m_A}\right|, \left|\tau_{12}^{m_B}\right|$) is $\geq$ than the matrix shear strength.
- Matrix cracking in transverse tension occurs when the max of ($\left|\sigma_{22}^{m_A}\right|, \left|\sigma_{22}^{m_B}\right|$) is $\geq$ than the tensile strength of the matrix material.
- Matrix cracking in transverse compression occurs when the max of ($\left|\sigma_{22}^{m_A}\right|, \left|\sigma_{22}^{m_B}\right|$) is $\geq$ than the compression strength of the matrix material.
- Matrix cracking in axial tension occurs when the max of ($\left|\sigma_{11}^{m_A}\right|, \left|\sigma_{11}^{m_B}\right|$) is $\geq$ than the tensile strength of the matrix material.
- Matrix cracking in the transverse direction occurs when the max of ($\left|\sigma_{13}^{m_A}\right|, \left|\sigma_{13}^{m_B}\right|$) or ($\left|\sigma_{23}^{m_A}\right|, \left|\sigma_{23}^{m_B}\right|$) is $\geq$ the shear strength of the matrix material.
- Fiber micro buckling resulting in Kink-Banding occurs when $\left|\sigma_{11}\right|_{La\,\min\,ate} \geq V_f G_{12T}$. Where $V_f$ is the fiber volume fraction and $G_{12T}$ is the tangent shear modulus.

Delamination failure is not modeled since normal stresses are ignored in shell formulations.

Figure 1. Outline of analysis procedure

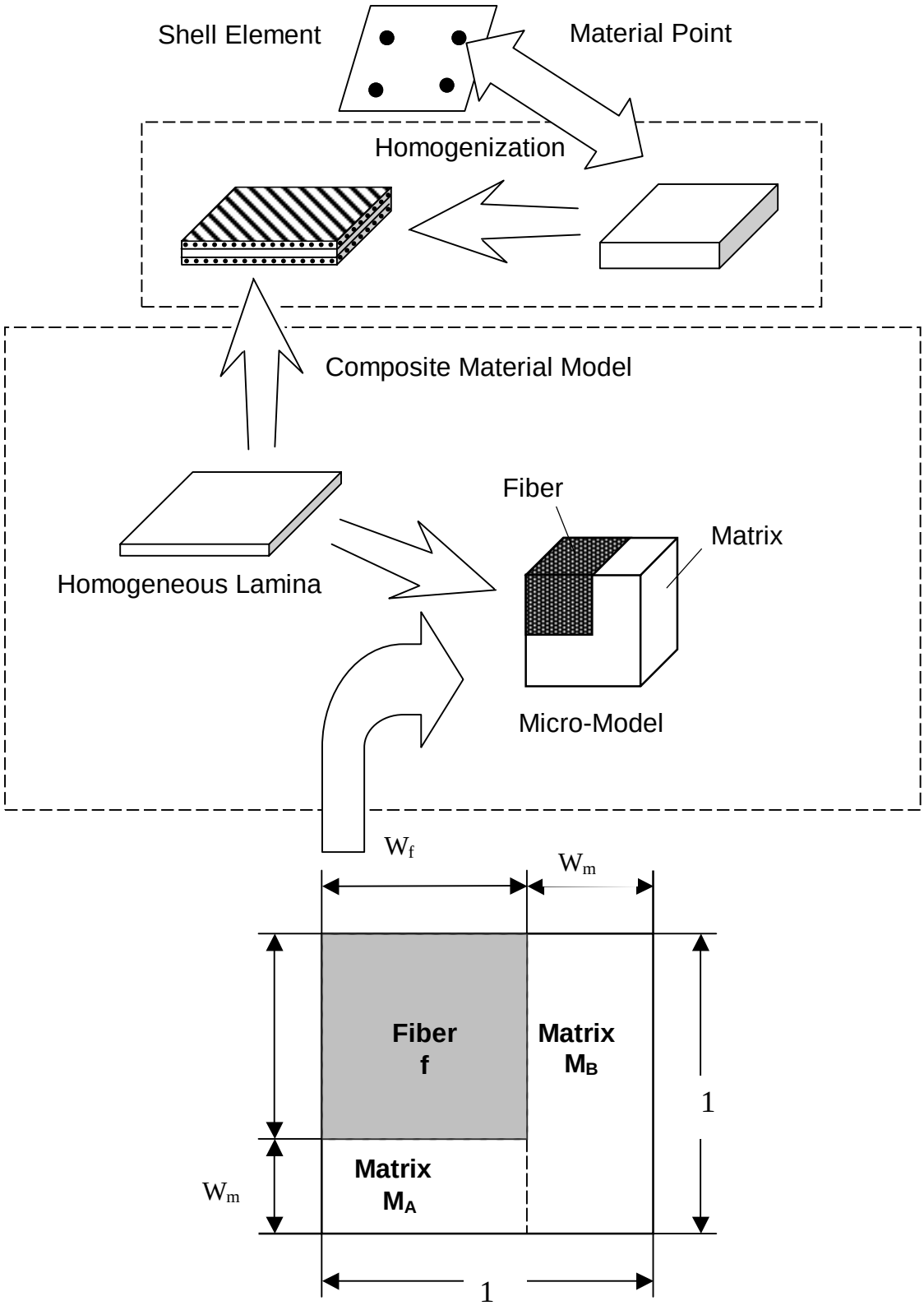

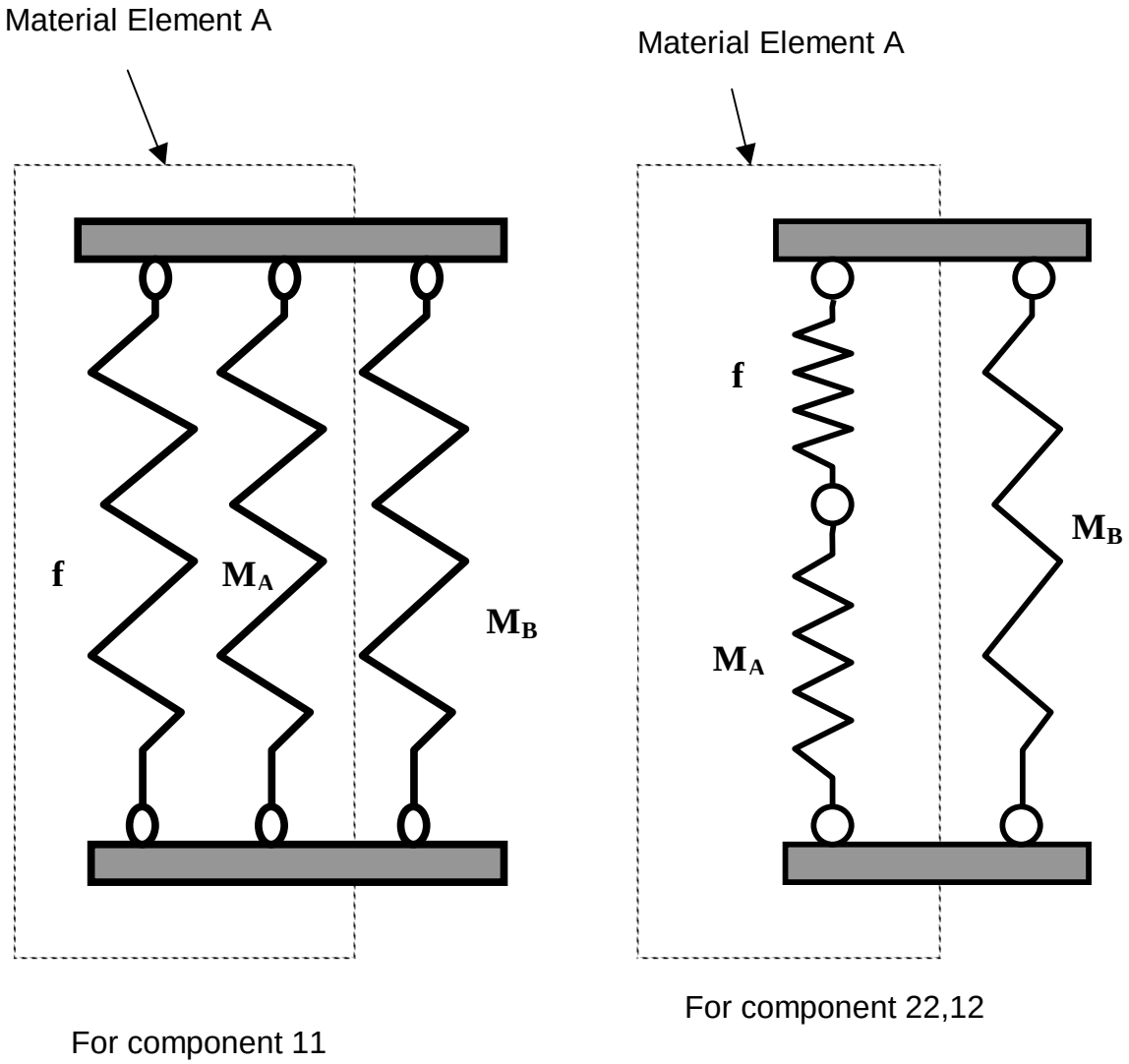


Figure 2. Analogy for stress and strain homogenization in the unit cell

**Results and Discussion**

The developed micro-mechanics constitutive equations are implemented in the explicit finite element method. The micro failure criteria (MFC) are also defined in the implemented constitutive equations. To demonstrate the applicability of the developed solution methodology for numerical simulation, several examples are presented for the validation of the material model. One of the examples demonstrates the advantage of the micro mechanics material model in the sense that fiber volume fraction can be altered and results can be obtained in which is not possible in macro mechanics models. Another example demonstrates the applicability of the developed material model for crashworthiness simulations.

Table (1) lists the mechanical and strength properties of a typical laminated Graphite/Epoxy composite materials. In the above table properties are presented for a lamina. However, in using the developed constitutive equations properties of the constituents are needed and called by the material model. Tables (2-4) lists the mechanical and strength properties of the constituent materials namely fiber and matrix for Graphite/Epoxy, Boron/Epoxy, and Kevlar/Epoxy composites.

Several test cases are considered for validation of the implementation of the model in the explicit finite element code DYNA3D. Finite element model of a coupon test is developed and simulated under tension as depicted in figure (3). Figure (4) depicts the ultimate load carried by the specimen. The material properties in tables (2-4) are considered for three tension test simulation of the coupon. Prediction of the material model and theory for the axial strength of the three materials is presented in table (5). Figure (5) depicts the same specimen under tension with various fiber volume fractions for Graphite/Epoxy composite. As expected the ultimate load carrying capacity of the specimen increases as the fiber volume fraction increases. The model is used to predict the experimental behavior of the IM7/977-2 composite in the longitudinal and transverse direction. Material and strength properties of the IM7/977-2 composite are listed in table (6). Figures (6) and (7) depict the prediction of the implemented material model versus experimental data for the ($0^o$) and ($90^o$) respectively. To verify the implementation of the failure criterion a finite element model is generated as depicted in figure (8). Various loads applied in different directions to invoke certain failure modes. Failure modes in the longitudinal fiber direction, transverse direction, shear direction, compressive fiber direction, and compressive transverse direction are considered. Results for a central element in the finite element model are presented for the various failure modes in figures (9-13). These results are summarized and compared to the experimental data in table (7).

A finite element model of a quasi-isotropic square tube is developed to simulate axial crash. Figure (14) depict one quarter of the square tube with several crash initiators. The composite tube is assumed to be fixed at the end and impacted by a rigid wall. Figure (15) depicts the crash force as a function of time. As can be seen from the presented examples, the developed solution methodology for the explicit finite element method yield stable solution and can be used for crashworthiness and impact simulation.

**Conclusion**

Micro-mechanical material model is defined for the explicit finite element method. A stress update procedure is developed and stress/strain-averaging procedure is presented for predicting the behavior of laminated composites on the micro level. The presented methodology is directly applied to nonlinear explicit finite element codes for structural analysis as demonstrated in the investigation. The progressive failure in the composite material can be captured with high level of confidence provided that experimental characterization is performed. This is accomplished by defining Micro-Failure Criteria (MFC) for determination of the various failure modes since stresses and strains in each sub-cell and

each constituent is available at each time step and load increment. Validation of the implemented model is presented in this study. The model is proven to be adequate and efficient for explicit finite element simulations.

## Refrences

[1] Bahei-El-Din, Dvorak, G. j. and Utku, S., "Finite element analysis of elastic-plastic fibrous composite structures, " Computers and Structures, Vol. 13, 1981, p.321-330.
[2] Adams, D. f. and Crane, D. A., "Finite Element Micro-mechanical Analysis of Unidirectional Composite Including Longitudinal Shear Loading, " Computers and Structures, Vol. 18, 1984, p.1153-1165.
[3] Pecknold, D. A. and Rahman S., "Micromechanics-based structural analysis of thick laminated composites", Report UILU-ENG-92-2012, ISSN 0069-4274, 1992, also see Computers & Structures, Vol. 51, 1994, p. 163-179.
[4] Chang, Fu-Kuo and Lessard, L. B., "Damage Tolerance of Laminated Composites Containing an Open Hole and Subjected to Compressive Loading", J. of Composite Materials, Vol. 25, 1991, p. 2-43.
[5] Tabiei, A., Jiang, Y. and Simitses, G. J., "Compressive Behavior of Moderately Thick Plates with Progressive Damage", Mechanics of Composite Materials and Structures, Vol. 4, 1997, p.281-295.

## Acknowledgment

Computing support was provided by the Ohio Super Computer Center. Their Support is greatly appreciated. The principle author would like to extend sincere thanks to the Lawrence Livermore National Laboratory (LLNL) for providing the source codes for DYNA3D.

Table 1. Properties of typical unidirectional composite material (unit: MPa)

| | AS/3501 Graphite/Epoxy | B(4)/5505 Boron/Epoxy | Kevlar/Epoxy |
|---|---|---|---|
| $E_x$ | 138000 | 204000 | 76000 |
| $E_y$ | 8960 | 18500 | 5500 |
| $\nu_{xy}$ | 0.3 | 0.23 | 0.34 |
| $G_{xy}$ | 7100 | 5590 | 2300 |
| Density, (ton/mm$^3$) | 1.6e-9 | 2.0e-9 | 1.46e-9 |
| $X_t$ | 1447 | 1260 | 1400 |
| $X_c$ | 1447 | 2500 | 235 |
| $Y_t$ | 51.7 | 61 | 12 |
| $Y_c$ | 206 | 202 | 53 |
| S | 93 | 67 | 34 |
| $V_f$ | 0.66 | 0.5 | 0.60 |

Table 2. Properties of Graphite/Epoxy for each constituent

| | $E_1$ (GPa) | $E_2$ (GPa) | $\nu_{12}$ | $\nu_{23}$ | $G_{12}$ (GPa) | $Xt^{(f)}$ (MPa) | $Yt^{(m)}$ (MPa) | $S^{(m)}$ (MPa) |
|---|---|---|---|---|---|---|---|---|
| Graphite | 213.7 | 13.8 | 0.2 | 0.25 | 13.8 | 2250 | _____ | _____ |
| Epoxy | 3.45 | 3.45 | 0.35 | 0.35 | 1.3 | _____ | 62.9 | 108 |

Table 3. Properties of Boron/Epoxy constituent

| | $E_1$ (GPa) | $E_2$ (GPa) | $\nu_{12}$ | $\nu_{23}$ | $G_{12}$ (GPa) | $Xt^{(f)}$ (MPa) | $Yt^{(m)}$ (MPa) | $S^{(m)}$ (MPa) |
|---|---|---|---|---|---|---|---|---|
| Boron | 400 | _____ | 0.2 | | 166.7 | 2566 | _____ | _____ |
| Epoxy | 3.45 | 3.45 | 0.35 | 0.35 | 1.3 | _____ | 62.9 | 108 |

Table 4. Properties of Kevlor/Epoxy constituent

| | $E_1$ (GPa) | $E_2$ (GPa) | $\nu_{12}$ | $\nu_{23}$ | $G_{12}$ (GPa) | $Xt^{(f)}$ (MPa) | $Yt^{(m)}$ (MPa) | $S^{(m)}$ (MPa) |
|---|---|---|---|---|---|---|---|---|
| Kevlar | 124.1 | 4.1 | 0.35 | 0.35 | 2.9 | 2031 | _____ | _____ |
| Epoxy | 3.45 | 3.45 | 0.35 | 0.35 | 1.3 | _____ | 62.9 | 108 |

Table 5. Axial tensile strength from micro-model and theory prediction.

| | Xt from micro-model | Xt from theory | Error |
|---|---|---|---|
| AS/3501 | 1498 Mpa | 1506 Mpa | -1.5% |
| Boron/Epoxy | 1362 Mpa | 1300 Mpa | 4.8% |
| Kevlar/Epoxy | 1171 Mpa | 1241 Mpa | -5.6% |

Table 6. Material properties of “IM7/977-2” composite

| | Longitudinal Modulus (Gpa) | Transverse Modulus (Gpa) | Poisson’s Ratio | In-plane Shear Modulus (Gpa) |
|---|---|---|---|---|
| Matrix 977-2 | 3.65 | 3.65 | 0.4 | 1.3 |
| Fiber IM-7 | 276 | 13.8 | 0.25 | |
| | Tensile strength | | Compressive strength | Shear strength |
| Matrix 977-2 | 90 Mpa | | 180 Mpa | 80 Mpa |
| Fiber IM-7 | 4040 Mpa | | --- | --- |

Table 7. Prediction versus experiment for T300/BP976 composites [ksi]

| | Tension in transverse direction $Y_t$ | Tension in fiber direction $X_t$ | Shear direction stress $S$ | Compression in fiber direction $X_c$ | Compression in transverse direction $Y_c$ |
|---|---|---|---|---|---|
| Experiment [3] | 6.5 | 220.0 | 15.5 | 231.0 | 37.0 |
| Prediction | 6.27 | 207.5 | 14.3 | 527.2 | 35.3 |

Figure 3. Finite element model of the specimen

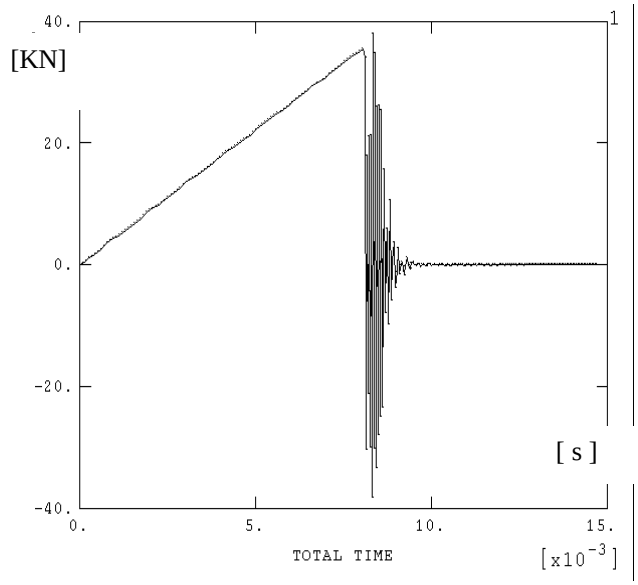


Figure 4. Ultimate axial tension load for AS/3501 ($0^o/0^o/0^o/0^o/0^o/0^o$)

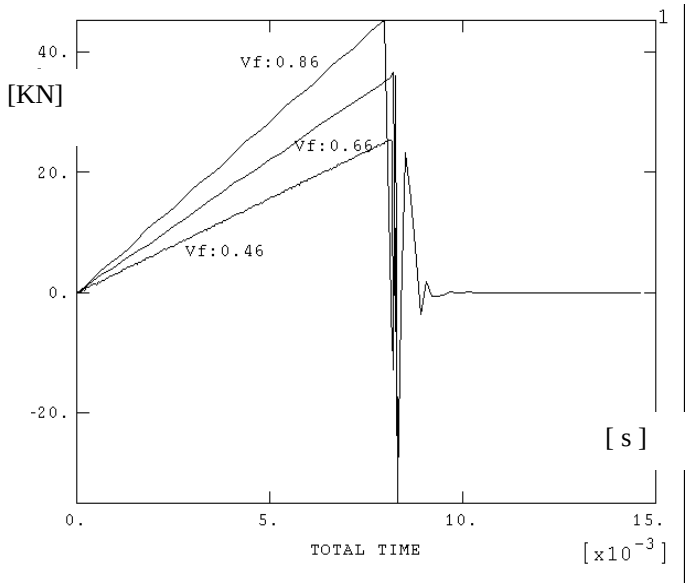


Figure 5. Fiber volume fraction effect on ultimate axial tension load for AS/3501 ($0^o/0^o/0^o/0^o/0^o/0^o$)

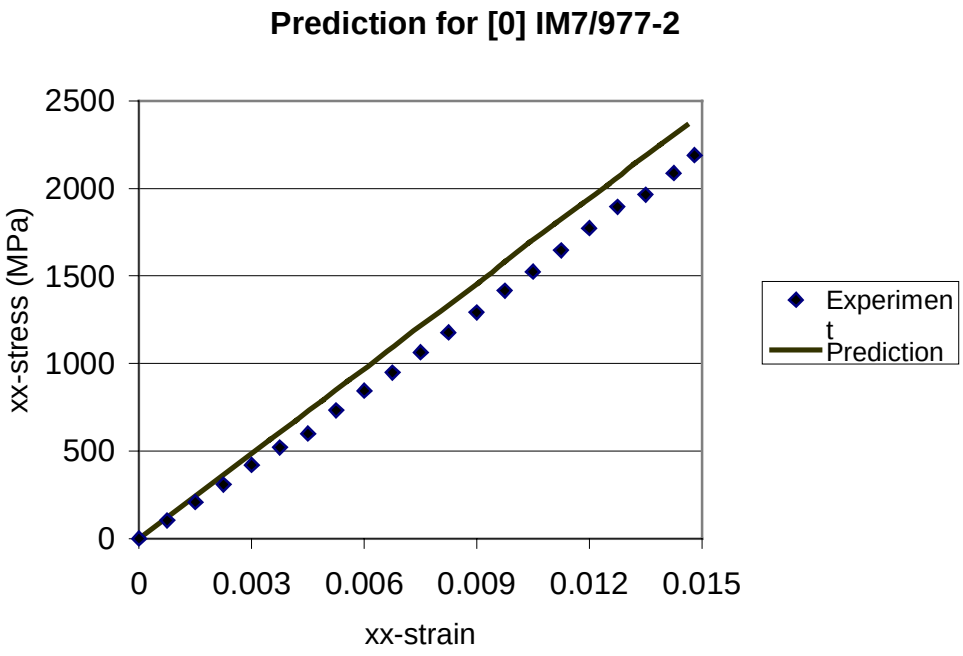


Figure 6. Experimental results and model prediction for (0-degree) composite

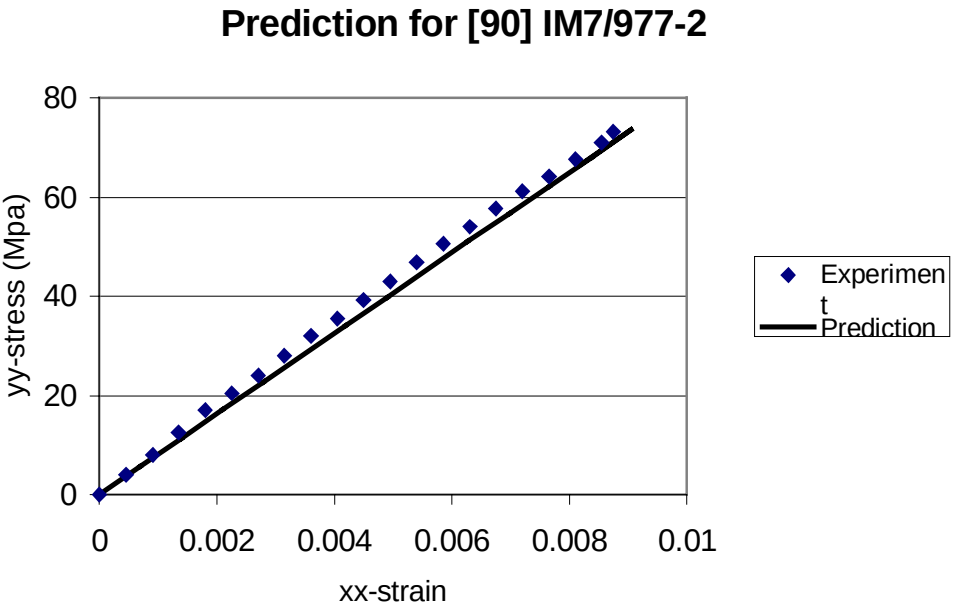


Figure 7. Experimental results and model prediction for (90-degree) composite

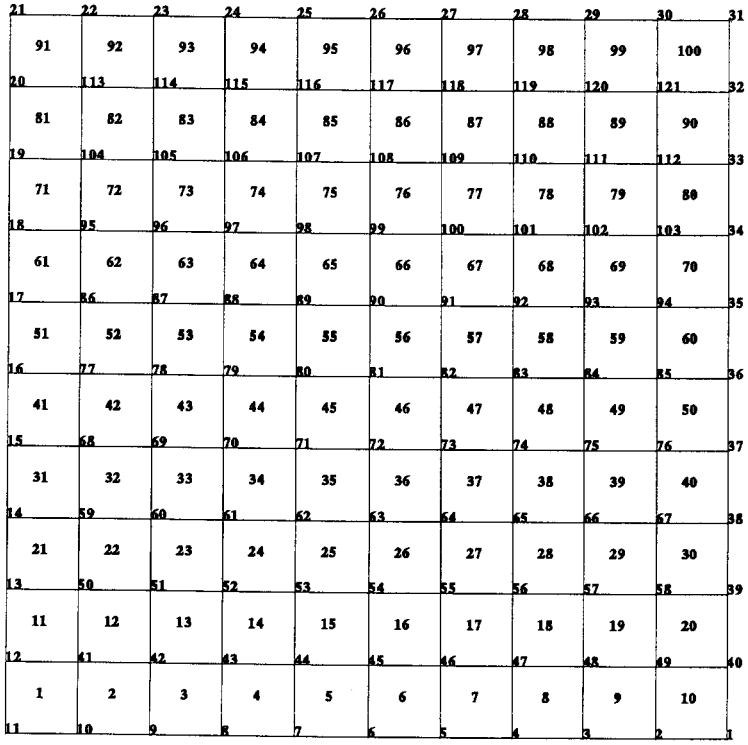


Figure 8. Finite element mesh of the validation model

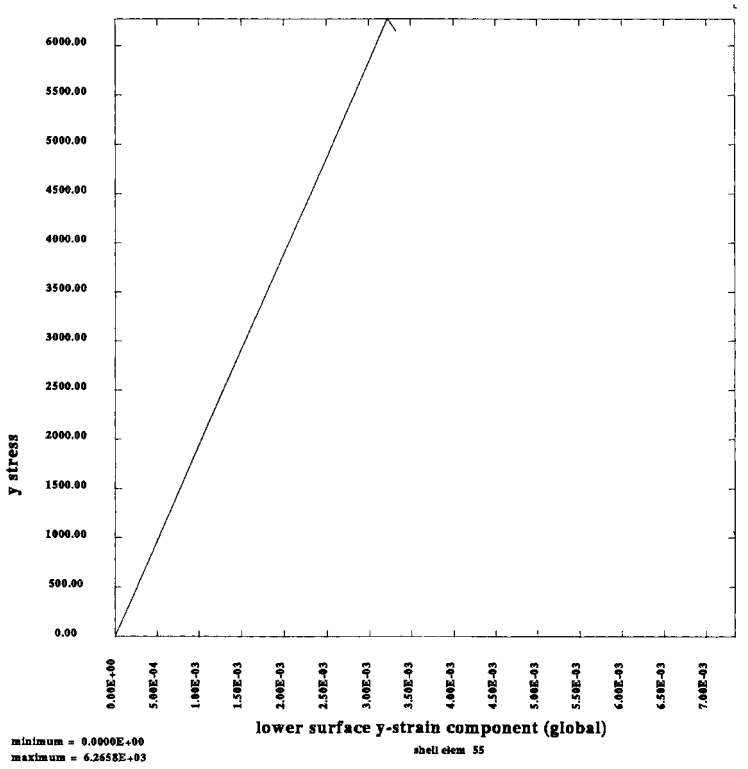


Figure 9. Tension in transverse direction

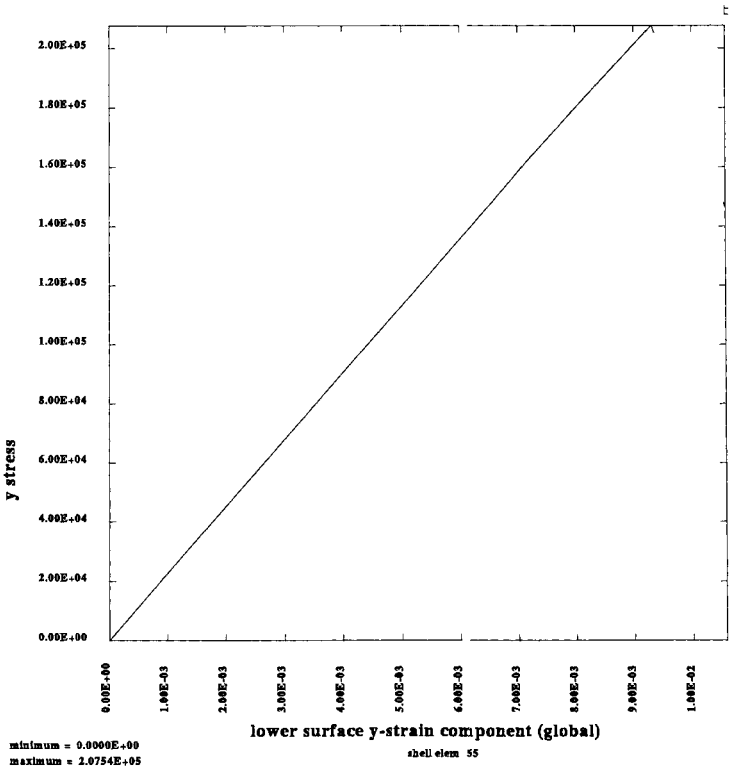


Figure 10. Tension in the fiber direction

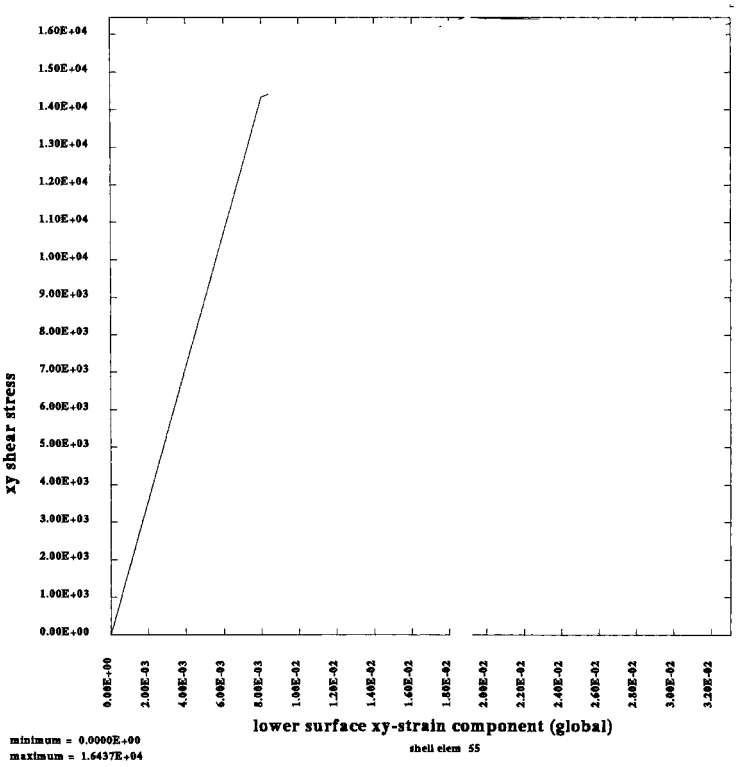


Figure 11. Shear stress

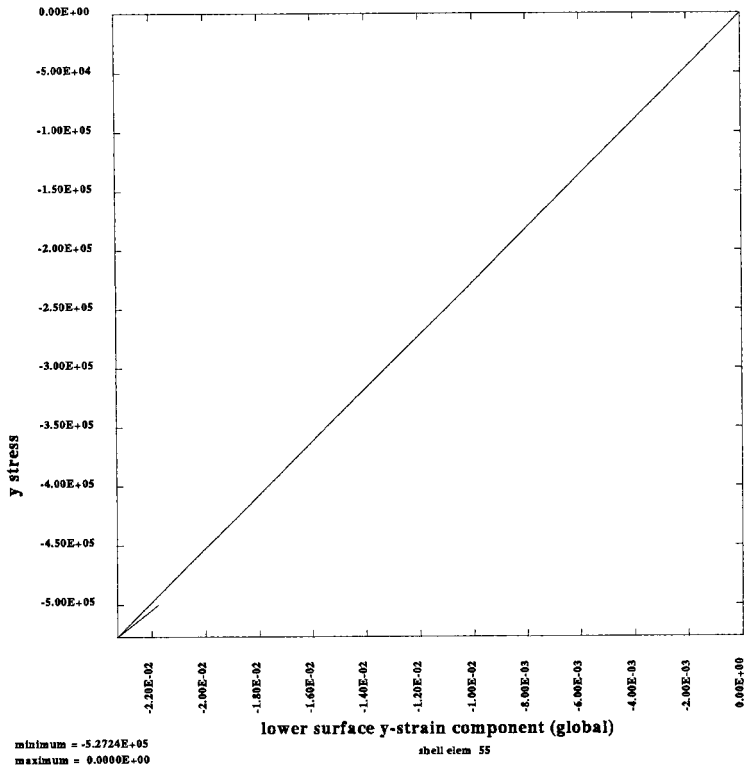


Figure 12. Compression in fiber direction

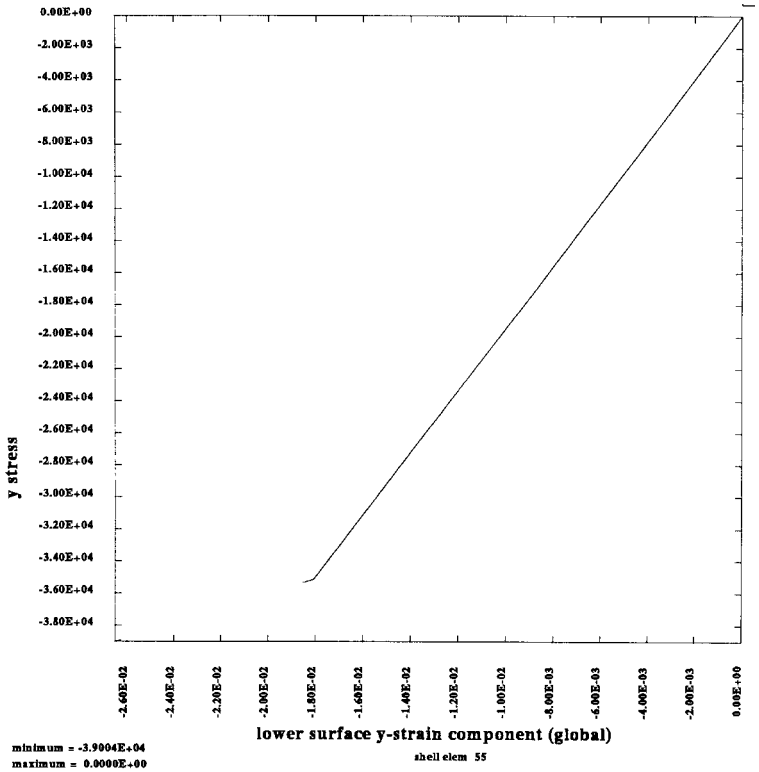


Figure 13. Compression in the transverse direction

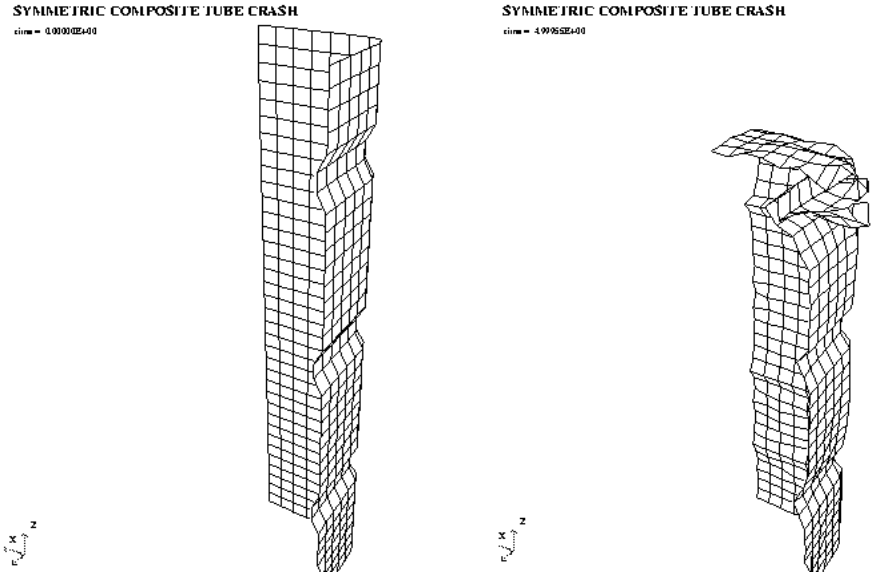


Figure 14. Crash of AS/3501 ($0^o$/-$45^o$/$45^o$/$90^o$/$90^o$/$45^o$/-$45^o$/$0^o$) composite tube

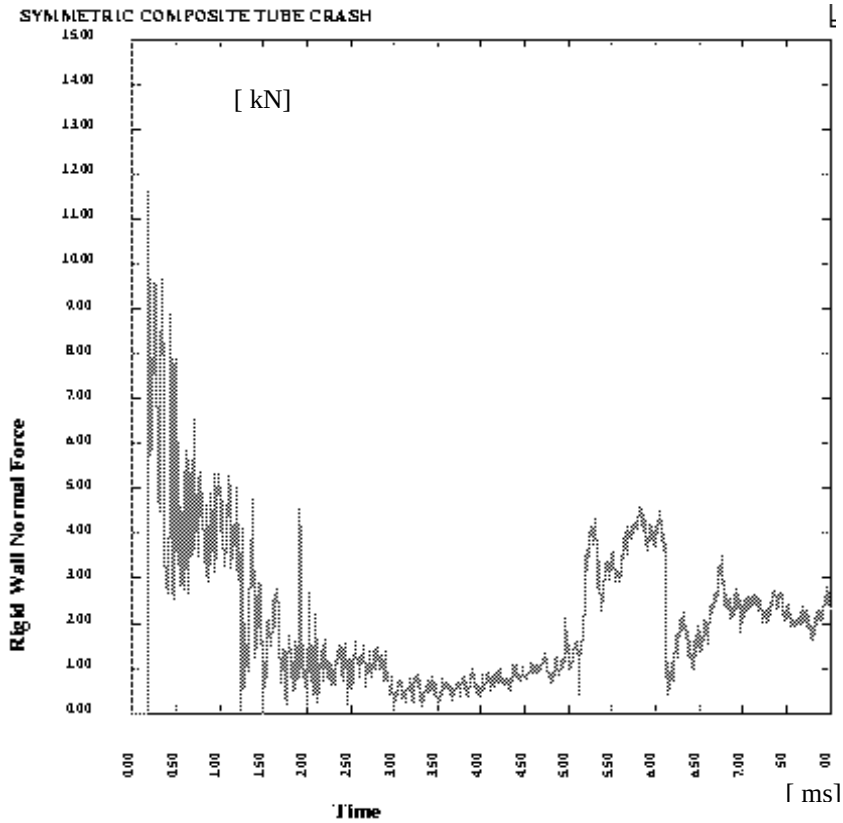


Figure 15. Crash force of AS/3501 ($0^o$/-$45^o$/$45^o$/$90^o$/$90^o$/$45^o$/-$45^o$/$0^o$) composite tube